Springer

KSME

Journal of Mechanical Science and Technology 29 (1) (2015) 397~407
www.springerlink.com/content/1738-494x
DOI 10.1007/s12206-014-1246-4

Virtual excavator simulator featuring HILS and haptic joysticks †

Yun-Joo Nam[1] and Myeong-Kwan Park[2,*]

[1]*Korea Institute of Industrial Technology, Cheonan, 331-822, Korea*
[2]*Department of Mechanical Engineering, Pusan National University, Busan, 609-735, Korea*

(Manuscript Received September 13, 2013; Revised July 17, 2014; Accepted July 31, 2014)

Abstract

This paper presents a virtual excavator simulator featuring hardware-in-the loop-simulation (HILS) technology and haptic joysticks. First, the technical concept of the virtual excavator simulator is proposed. Then, the mathematical relations describing the behavior of the excavator are derived for the software environment. Next, for reflecting the nonlinear and dynamic characteristics of the hydraulic system in the excavator, the simulation software is integrated with the hydraulic system hardware. In addition, for improving the interaction performance between the operator and the simulator, MR fluid actuator based haptic joysticks are employed. The experimental performance evaluation verified that the proposed concept of the virtual excavator simulator is effective and practical from the viewpoint of the reality improvement.

Keywords: MR rotary actuator; Haptic joystick; HILS (hardware-in-the loop-simulation); Virtual excavator simulator

1. Introduction

Hydraulic excavators are widely used in construction, agricultural, forestry, and mining industries, due to their kinematic flexibility and high power density. The excavator operation is mostly executed by skillful operators who manipulate hydraulic joysticks to drive multiple links. Because of harsh working environment and physical fatigue from long working time, the excavator operation is avoided. Also, the excavator operation by the intuition of the operator always includes potential risk caused by lack of skill and mistakes. Therefore, many researchers have focused on intelligent, autonomous or robotic excavator systems.

Multi-sensing and signal processing technologies for detecting excavator motion and working environment have been investigated. Bernold et al. proposed a 3-D mapping methodology of working terrain by using two sensors, EMI (electromagnetic induction) and GPR (ground penetrating radar), which are installed on the bucket [1]. Lever et al. mounted force and torque sensors on the bucket joint to control the excavator motion and developed a fuzzy logic algorithm to process multiple sensing signals [2]. Stentz et al. developed a perception system using a laser, a camera and proprioceptive sensing elements for the unmanned ground vehicle system to detect and avoid obstacles in natural terrain environment [3]. In addition, the control algorithms for autonomous excavator have been researched. Koivo et al. presented a dynamic model of the excavator based on the modified Newton-Euler method and adopted the proportional-differential controller to compensate the tracking errors due to the external forces applied to the bucket [4]. He et al. proposed a tracking controller by considering the dynamic characteristics of hydraulic systems [5]. Ha et al. proposed a robust sliding mode controller for the impedance control of the excavator and verified the tracking performance experimentally [6]. However, difficult information correlation and complex control algorithm have still many limitations in field applications.

Recently, to overcome the limitations of excavator automation, many researches on tele-operation technology and simulators have been carried out. In the tele-operation system, the operator is spatially separated from the operating excavator by using the master-slave system, and hence, can be excluded from potential hazard in the working environment. Especially, the haptic interfaces for force reflection have been presented to improve the reality shortage resulting from unilateral information transmission of the existing joysticks. The force feedback provides the operator with useful information for flexible operation of the excavator and safety of themselves. Parker et al. designed the force-reflecting controller using 6-DOF maglev joysticks, for the rate control of the hydraulic system in conventional heavy machines [7]. Frankel et al. used the commercially available haptic user interface, PHANToM 1.0, as the master device and the excavator as the slave machine, in order to evaluate the performance of the proposed haptic control algorithm [8]. Takemoto et al. developed a

*Corresponding author. Tel.: +82 51 510 2464, Fax.: +82 51 514 0685
E-mail address: mkpark1@pusan.ac.kr
† Recommended by Associate Editor Jae Cheon Lee

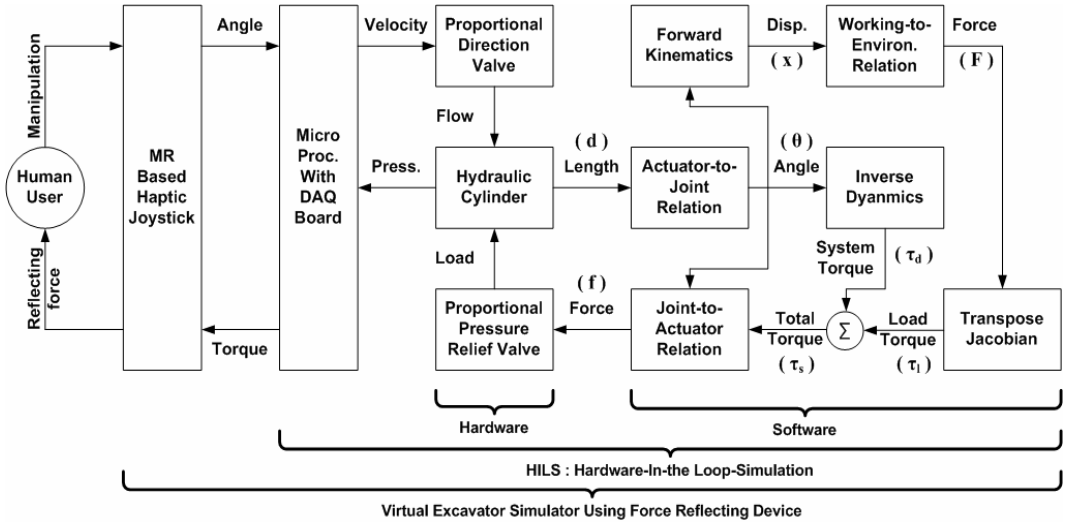

Fig. 1. Schematic diagram of the virtual excavator simulator.

semi-automatic man-machine system using the 2-DOF haptic joystick based on AC servo motor, for operating the rotary crane [9]. However, haptic instability and interface danger resulting from active actuators, such as motor or hydraulic cylinder, still remain to be solved in the haptic interface.

On the other hand, many researches on excavator simulators based on the software environment have been conducted for tele-operation and operator training system. Yang et al. developed an excavator simulator using the commercial software, AMESim, for modeling the hydraulic system [10]. DiMaio et al. presented a simulator consisting of the impedance model of the excavator, the bucket-ground interaction model, the graphically rendered environment and the haptic interface, in order to evaluate the training performance for operators and the control strategies for heavy-duty hydraulic machines [11]. Toreres-Rodiquez et al. proposed a force-position control algorithm and auto-balanced haptic interfaces for training the excavator operator [12]. However, it is difficult to model the hydraulic system in the simulation environment due to its strong nonlinearity. Also, the computation burden due to the complex mathematical relations degrades real-time control performance. To overcome these drawbacks, HILS (hardware-in the-loop-simulation) technology can be considered to replace the simulation software with the hydraulic system hardware.

Consequently, we propose a virtual excavator simulator consisting of simulation environment, HILS technology and passive actuator based haptic interfaces. In the simulation environment, the mathematical relations describing the behavior of the excavator do not have to be solved by numerical analysis. Instead, the relations are the kinematics and dynamics with the closed solutions, which makes the real-time implementation possible. The HILS system is adopted to reflect the nonlinearity and the dynamic characteristics of the hydraulic system to the simulation loop. The modeling errors due to parameter uncertainty and complex nonlinearity can be minimized and the real time control performance can be assured by the real hydraulic system. MR fluid based haptic joysticks are developed for improving the manipulation sensation of the operator by the bilateral information transmission between human users and machines. The control stability and the interface safety can be assured simultaneously by the passive actuator. Through the experimental performance evaluation, it is verified that the proposed concept of the virtual excavator simulator is effective and practical in the viewpoint of reality improvement.

2. Concept of the virtual excavator simulator

Fig. 1 shows the technical concept of the virtual excavator simulator. When the human user manipulates the haptic joystick, the joystick angles detected by the rotary encoders are converted to the velocity control inputs to the proportional direction control valves via DAQ for operating the hydraulic cylinders in the HILS system. The cylinder lengths measured by the displacement transducers are inputted to the software environment as the cylinder lengths in the virtual excavator and used to obtain the revolute joint angles from the cylinder length-to-revolute joint angle relationship. The obtained joint angles are used as the inputs of the inverse dynamics to obtain the system torques applied to the revolute joints by the inertia and weight of the excavator itself during the operation. Also, they are used as the inputs of the forward kinematics to find the positions and orientation of the bucket tip. Then, the external loads applied to the bucket tip are obtained from the bucket tip position information and the working environment model describing the relationship between the soil and the bucket tip during digging operation. The loads applied on the joints are determined by the external loads and the transposed Jacobian matrix of the excavator. The total torque, which is a

combination of the system torques and the load torques, and the joint angles are input to the joint-to-actuator force relation to obtain the cylinder force of the virtual excavator. The cylinder forces are used as the pressure control inputs to the proportional pressure relief valves, and then the corresponding load pressures are applied to the hydraulic cylinders in the HILS system. The load pressures are measured by the pressure transducers on the cylinders and converted to the torque control inputs to the MR rotary actuators installed on the haptic joysticks via DAQ board. As a result, the human user can perceive the torque outputs of the haptic joysticks corresponding to the load pressures in the hydraulic cylinders.

The software environment for the virtual excavator simulator is 2-D graphical simulation based on the kinematics and dynamics of the excavator itself. The mathematical model of the hydraulic system actually has strong nonlinearity in the valve orifice flow equation and in the simultaneous nonlinear differential equations. Also, the working oil properties, such as viscosity, density and compressibility, vary according to the working environment, leading to parameter uncertainty in the hydraulic system model. To present more realistic manipulation, the real hydraulic system hardware is integrated to the simulation software via HILS technology. The dynamic characteristics of the hydraulic system due to the nonlinearity and the uncertainty are considered effectively. On the other hand, the haptic joysticks for the bilateral information transmission between the human user and the machine provide the operator with the force feedback corresponding to the dynamic load of the virtual excavator. The active actuators in most of the conventional haptic interfaces have the limitation of control instability due to the information delay in remote communication as well as of the undesired chattering phenomenon due to the feedback control algorithm. Also, from the viewpoint of interface safety, undesired or sudden operation of the active actuator by wrong input signal can give physical injury or uneasy mind to the operator. To overcome these limitations of the active actuator, the MR fluid actuators providing only the reaction force against the manipulation of the operator are adopted for the haptic interface. Due to the passivity property of the MR actuator, the haptic stability and the interface safety are guaranteed simultaneously.

3. Excavator modeling

3.1 Coordinate systems

Disregarding the swing motion, the excavator manipulator can be considered as a planar 3-DOF serial mechanism. To describe the behavioral characteristics of the excavator, the forward kinematics, the cylinder actuator-to-revolute joint relations, the inverse dynamics, the velocity/force transmission characteristics and the working environment model are required. For modeling the excavator, four coordinate systems are introduced, as shown in Fig. 2. Here, $\{O_i\}$ is the i^{th} coordinate system, d_i is the i^{th} hydraulic cylinder length, θ_i is the revolute joint angle corresponding to the i^{th} hydraulic cylinder,

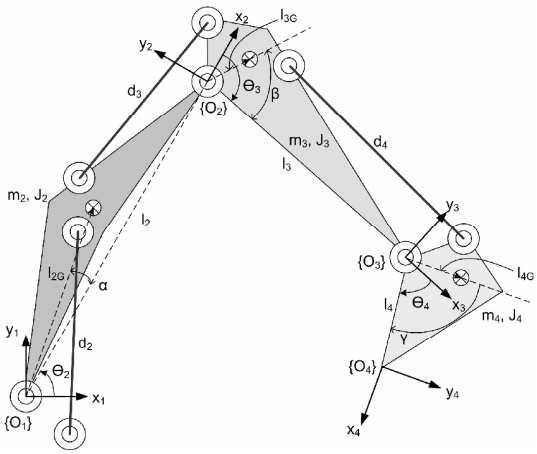

Fig. 2. Coordinate systems of the excavator.

l_i is the distance between the origins of the $(i\text{-}1)^{th}$ and i^{th} coordinate systems, l_{iG} is the distance between the origin of the $(i\text{-}1)^{th}$ coordinate system and the center of mass of the i^{th} link. m_i and J_i represent the mass and inertia moment of the i^{th} link, respectively. α, β and γ are the geometric parameters representing the angle between l_i and l_{iG}.

3.2 Forward kinematics

The forward kinematic of the excavator is defined as the problem to find the positions and orientation of the bucket tip when the revolute joint angles are given. From the homogeneous transformation matrices describing the relationships between the adjacent joints, the posture of the bucket are obtained from the given joint angles, as follows

$$x = l_2\cos\theta_2 + l_3\cos(\theta_2-\theta_3) + l_4\cos(\theta_2-\theta_3-\theta_4)\,, \quad (1)$$

$$y = l_2\sin\theta_2 + l_3\sin(\theta_2-\theta_3) + l_4\sin(\theta_2-\theta_3-\theta_4)\,, \quad (2)$$

$$\Theta = \theta_2-\theta_3-\theta_4\,, \quad (3)$$

where x, y and Θ are the positions and orientation of the bucket tip with respect to the reference coordinate system $\{O_1\}$, respectively.

3.3 Actuator-to-joint position relation

The configuration of the excavator manipulator is determined by the revolute joint angles corresponding to the hydraulic cylinder length. As shown in Fig. 3, the relationships between the hydraulic cylinder length d_i and the revolute joint angle θ_i are given by

$$\theta_i = \cos^{-1}\left[\frac{a_i^2+b_i^2-d_i^2}{2a_ib_i}\right]-(\pi-\theta_{i0}-\theta_{i1}) \quad (i=2,3,4)\,, \quad (4)$$

where a_i, b_i, θ_{i0} and $\theta_{i1}(i = 2, 3, 4)$ are the geometric parameters of the excavator. Since the relation for the linkage con-

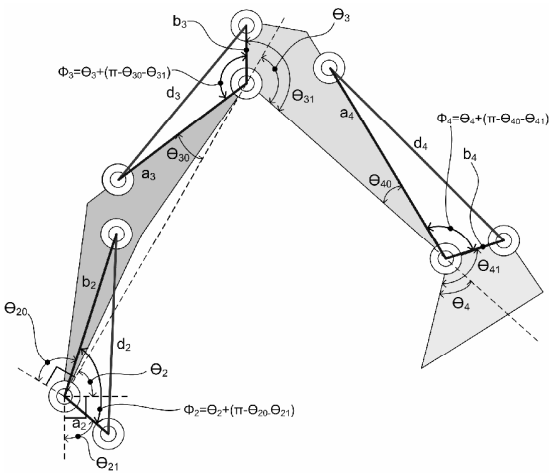

Fig. 3. Cylinder-joint relations.

necting the bucket cylinder and bucket itself does not require complicated kinematics and dynamics, the expansion of the relation does not have a negative effect on the real-time implementation. Therefore, in this study, the relation of the attachment coupler is omitted for the sake of convenience.

3.4 Velocity/force transmission characteristics

The velocity transmission characteristic of the excavator manipulator representing the bucket output velocity with respect to the joint input velocity is obtained by differentiating the forward kinematics (1) to (3), as follows:

$$\dot{\mathbf{x}} = \mathbf{J}\dot{\boldsymbol{\theta}}\,, \tag{5}$$

where $\boldsymbol{\theta} = [\theta_2,\ \theta_3,\ \theta_4]^{\mathrm{T}}$ is the rotational velocity of the joints, and $\mathbf{x} = [x,\ y,\ \Theta]^{\mathrm{T}}$ is the velocity of the bucket tip. The velocity Jacobian is given by

$$\mathbf{J} = \begin{bmatrix} -l_2 s\theta_2 - l_3 s\theta_\alpha - l_4 s\theta_\beta & l_3 s\theta_\alpha + l_4 s\theta_\beta & l_4 s\theta_\beta \\ l_2 c\theta_2 + l_3 c\theta_\alpha + l_4 c\theta_\beta & l_3 c\theta_\alpha + l_4 c\theta_\beta & l_4 c\theta_\beta \\ 1 & -1 & -1 \end{bmatrix}, \tag{6}$$

where $\theta_\alpha = \theta_2-\theta_3$, $\theta_\beta = \theta_2-\theta_3-\theta_4$, $s(\cdot) = sin(\cdot)$ and $c(\cdot) = cos(\cdot)$. Then, the force transmission characteristic of the excavator manipulator representing the joint torque outputs with respect to the external load input applied to the bucket tip is obtained based on the principle of the virtual work, as follows.

$$\boldsymbol{\tau} = \mathbf{J}^T\mathbf{F}\,, \tag{7}$$

where $\mathbf{F} = [F_{ex},\ F_{ey},\ T_{ez}]^{\mathrm{T}}$ and $\boldsymbol{\tau} = [\tau_2,\ \tau_3,\ \tau_4]^{\mathrm{T}}$. τ_i is the joint torque corresponding to the i^{th} hydraulic cylinder actuator. F_{ex} and F_{ey} are the external forces applied to the bucket tip in the x and y-axis directions of the reference coordinate system, respectively. Considering the general working environment of the excavator, the external torque given at the bucket tip T_{ez} can be neglected ($T_{ez} = 0$). As a result, the load torques applied to the revolute joints, $\boldsymbol{\tau}_{\mathbf{l}}$, are determined by Eq. (7).

3.5 Actuator-to-joint velocity/force relation

The velocity transmission characteristic between the cylinder actuator input velocity and joint output velocity is obtained by differentiating Eq. (4), as follows.

$$\dot{\boldsymbol{\theta}} = \mathbf{J}_a\dot{\mathbf{d}}\,, \tag{8}$$

where $\mathbf{d} = [d_2,\ d_3,\ d_4]^{\mathrm{T}}$ is the actuator velocity. The velocity Jacobian of the actuators is given by

$$\mathbf{J}_a = diag\left(\frac{d_2}{a_2 b_2 \sin\varphi_2}, \frac{d_3}{a_3 b_3 \sin\varphi_3}, \frac{d_4}{a_4 b_4 \sin\varphi_4}\right), \tag{9}$$

where $\varphi_i = \theta_i+(\pi - \theta_{i0} - \theta_{i1})$. Then, the force transmission characteristic representing the actuator output force with respect to the joint input torque is

$$\mathbf{f} = \mathbf{J}_a^{\,T}\boldsymbol{\tau}\,, \tag{10}$$

where $\mathbf{f} = [f_2, f_3, f_4]^{\mathrm{T}}$ and f_i is the applied force to the i^{th} hydraulic cylinder actuator. Therefore, when the total torque combining the load and system torques, $\boldsymbol{\tau}_{\mathbf{s}}$, is given, the exerted forces by the cylinder actuators $\mathbf{f}$ are determined by Eq. (10).

3.6 Inverse dynamics

The inverse dynamics of the excavator manipulator is used to find the system torques applied to the revolute joints, $\boldsymbol{\tau}_{\mathbf{d}}$, when the joint angles and their derivatives are given. In other words, the inverse dynamics is defined as the problem to find the joint torques required for the behavior of the excavator manipulator. First, the translational and rotational kinetic energies at the center of mass of the links, V_{t} and V_{r}, are calculated. Next, the potential energy of the links, T, is found at the given configuration of the manipulator. Then, the dynamic governing relation of the excavator manipulator is obtained based on the Euler-Lagrangian method, as follows.

$$\frac{d}{dt}\left(\frac{\partial L}{\partial \dot{\theta}_i}\right) - \frac{\partial L}{\partial \theta_i} = \tau_{di} \quad (i = 2,\ 3,\ 4)\,, \tag{11}$$

where $L = V_{\mathrm{t}} + V_{\mathrm{r}} - T$ is the Lagrangian of the manipulator [4].

3.7 Working environment modeling

To define the external load applied to the bucket tip during the digging operation, the interaction relation between the bucket and the soil is required to be known. Since the relation has an effect on the properties of the soil itself as well as the

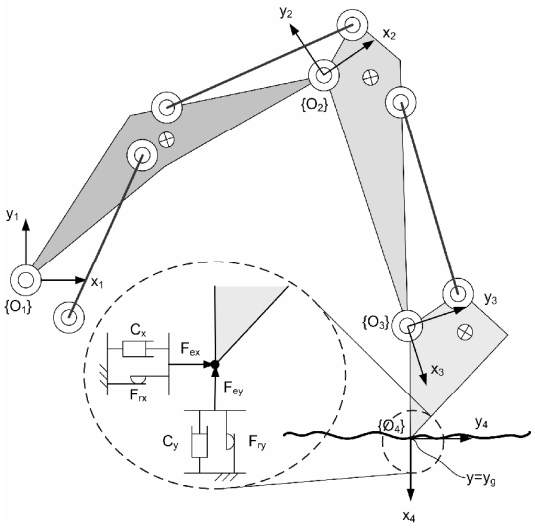

Fig. 4. Working environment modeling for the digging operation.

external conditions including moisture content, air density and temperature, it is very difficult to describe accurately. Young and Hanna developed the FEM that provides detailed information on the stress and deformation of the soil as well as the forces applied at the bucket, in order to study the performance of the flat blade moving in clay soil [13]. Luengo et al. presented a reformulated version of the classical fundamental equation of earthmoving in order to model the soil-bucket interaction, and developed an on-line method to estimate soil parameters from the force data measured at the bucket [14]. However, these studies still have limitations of modeling errors due to uncertainty and computational burden of complex modeling, in practical applications. Therefore, in this study, the external forces applied to the bucket by the soil are expressed by the combination of two mechanical elements representing viscosity and friction (Fig. 4).

$$F_{ex} = \begin{cases} C_x\dot{x} + F_{rx} & (y \le y_g) \\ 0 & (y > y_g) \end{cases}, \tag{12}$$

$$F_{ey} = \begin{cases} C_y\dot{y} + F_{ry} & (y \le y_g) \\ 0 & (y > y_g) \end{cases}, \tag{13}$$

where C_x and C_y are the coefficients of the viscosity in x and y direction of the reference coordinate system. F_{rx} and F_{ry} are the friction given as the constant. y_g is the position of the soil with respect to the reference coordinate system. The presented working environment model is very intuitive and effective for implementing the virtual excavator simulator. In other words, considering that the aim of this research is to propose the technical concept of the virtual excavator simulator, further study regarding the interaction between the soil and the bucket is of the next step for improving the practicability of the system.

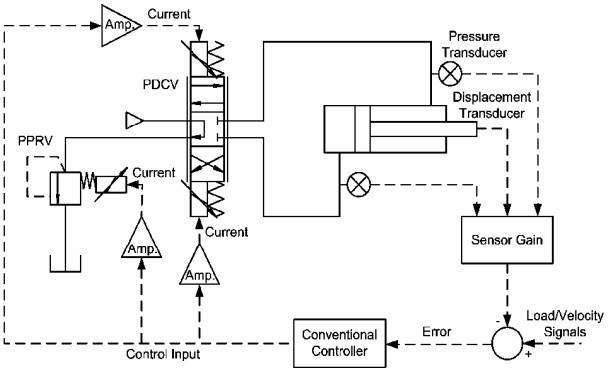

Fig. 5. Hydraulic circuit diagram for HILS.

4. HILS system

4.1 Hydraulic system hardware

In this study, the hydraulic system for the HILS technology is simplified rather than a real one in the aspect of size and capacity. Nevertheless, considering that nonlinearity and uncertainty of the hydraulic system are mainly caused by the valve orifice effect and the compressibility of the working oil, the proposed system is suitable to display the dynamic characteristics in real hydraulic system. In addition, the proposed hydraulic system presents an effective methodology for applying external loads to the hydraulic cylinder. In previous studies, the cylinder-to-cylinder configuration at which the position-controlled cylinder is connected to the force-controlled cylinder in series has been considered. However, the dynamic characteristics of the force-controlled system itself can give undesired effects to the position-controlled system.

The hydraulic circuit diagram of the proposed hydraulic system is shown in Fig. 5, where only one cylinder is represented, but the two other cylinders also have the same configuration. The proposed hydraulic system consists of a single-ended cylinder, a proportional direction control valve (PDCV), a proportional pressure relief valve (PPRV), two pressure transducers and a displacement transducer. The PDCV is installed between the pump and the cylinder and used to control the cylinder velocity corresponding to the haptic joystick angle. For more details, the maximum joystick angles are mapped to the maximum openings of the respective PDCVs. The cylinder displacement is measured by the displacement transducer. Since the PPRV is installed between the return port of the PDCV and the tank, the load pressure in the cylinder can be controlled correspondingly to the external loads applied to the bucket tip in the virtual environment. The load pressures are measured by two pressure transducers installed on both ports of the cylinder. As a result, the dynamic characteristics between the joystick angle input and the cylinder velocity output as well as between the external load input and the joystick force output can be effectively considered in the proposed HILS system.

Table 1. Design parameters of the virtual excavator simulator.

Boom		Arm		Bucket	
l_2	6200 mm	l_3	3050 mm	l_4	1570 mm
l_{2G}	2982 mm	l_{3G}	893.44 mm	l_{4G}	719.67 mm
α	0.208 rad	β	0.225 rad	γ	0.785 rad
m_2	2321 kg	m_3	1304 kg	m_4	1502.6 kg
J_2	10067.3 kgm^2	J_3	2111 kgm^2	J_4	360.4 kgm^2
a_2	900 mm	a_3	3139 mm	a_4	2335 mm
b_2	2587 mm	b_3	1010 mm	b_4	495 mm
θ_{20}	1.156 rad	θ_{30}	0.463 rad	θ_{40}	0.277 rad
θ_{21}	1.047 rad	θ_{31}	2.732 rad	θ_{41}	1.920 rad

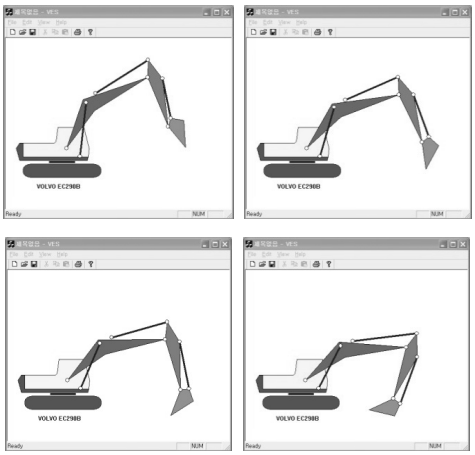

Fig. 6. Digging motion of the virtual excavator in the simulation.

4.2 Simulation environment software

To provide visual information on excavator behavior and working environment, the simulation environment is coded by VISUAL C++, as shown in Fig. 6. The main geometrical parameters for the excavator configuration are obtained from one of the commercially available excavators in 29 ton class, as presented in Table 1. The variables relating to the kinematics and dynamics of the excavator manipulator are considered in the software. In addition, the technical specifications and operation conditions of the hydraulic system hardware for the HILS are determined in the similarity to the virtual ones. The supply and load pressures in the HILS are specified at the level of 50% in the real system. The cylinder lengths and the piston cross-sectional areas in the HILS are chosen so that the piston can travel between two ends of the cylinder within the same time as the real system. In addition, the maximum angle input and maximum torque output in the haptic joysticks correspond to the maximum operation velocity and maximum load pressure in the hydraulic cylinders, respectively. In the working environment model, the viscosity coefficients C_x, C_y and the friction F_{rx}, F_{ry} are determined at 50% level of the maximum load pressure under the maximum operating velocity condition. The sampling interval for interfacing the hydraulic system and the haptic joysticks with the simulation software is set to 10 msec.

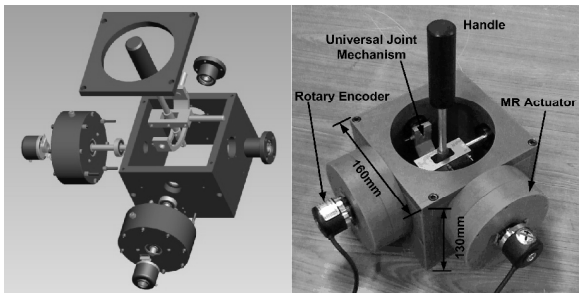

Fig. 7. Schematic of the haptic joystick.

5. Haptic joystick

5.1 Structure of the haptic joystick

The boom, arm, bucket and swing motions of the excavator are generally achieved by two 2-DOF hydraulic joysticks. For realizing the intuitive manipulation of the excavator, the 2-DOF haptic joysticks are proposed as shown in Fig. 7. The presented haptic joystick consists of a handle, a 2-DOF universal joint mechanism, two MR rotary actuators, two rotary encoders and a joystick body. The MR rotary actuator provides reactive torque output controlled by the coil current input. To detect the handle manipulator of the operator and to display the torque feedback to the operator, the 2-DOF universal joint mechanism is specially designed. The universal joint consists of two joint frame axes perpendicularly intersecting each other on common plane and one handle axis passing through the intersection of the frame axes. The one axis of the MR rotary actuators is connected to the join frame and supported by the ball bearing mounted on the joystick body. The other axis is connected to the hollow shaft typed rotary encoder for measuring the angular displacement of the joystick. The handle axis is constrained in the upper and lower frames by the pin and sliding connections, respectively. The slots in the frames are designed to make the handle freely move within the rotational range of ±40° with respect to the neutral position where the handle is placed in the gravity direction. Since the frame axes and the handle axis are intersected at the fixed point on the common plane, 2-DOF motion of the joystick handle is assured. The universal joint mechanism is made of aluminum and machined precisely to minimize the inertia and friction. The body of haptic joystick is made of MC nylon for considering its weight, strength and solidity.

5.2 MR rotary actuator

MR fluid is a non-colloidal solution composed of ferromagnetic particles with micrometers in diameter dispersed in a non-conductive carrier fluid. The MR fluid has the characteristic that its rheological property can be continuously and reversely changed within several milliseconds solely by apply-

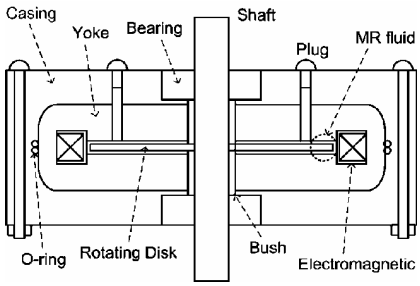

Fig. 8. Structure of the MR rotary actuator.

ing or removing external magnetic field. The devices using MR fluid can be made simple in construction, high in power, and low in inertia. Especially, the MR rotary actuator can provide safety in interface and stability in control for haptic devices interacting directly with the human user, due to its inherent stabilizing effect as a passive device. Considering that manipulation sensation of the excavator results from the resistance during digging operation, the application of the MR rotary actuator to the excavator simulator is very effective.

Fig. 8 shows the structure of the proposed MR fluid actuator. The gap between the rotary disk and two magnetic poles is filled with the MR fluid. The magnetic circuit of the MR fluid actuator consists of the MR fluid itself, the electromagnetic coil, and the yoke for forming the magnetic flux path. When the external current is supplied to the electromagnet coil by the current amplifier, the corresponding magnetomotive force is applied to the magnetic circuit and then, a magnetic field is generated in the MR fluid. Then, the dynamic yield stress of the MR fluid is changed depending on the magnetic field intensity, and the corresponding shear force is generated in the opposite direction of the rotary disk motion. As a result, the output torque of the MR fluid actuator can be continuously and reversely controlled by adjusting the coil current [15].

The output torques with respect to the rotational velocity (10~60 rpm) at various input currents (0~5A) are shown in Fig. 9(a). It is verified that the torque output is increased monotonically with the current input. In addition, the torque output is independent of the rotational velocity larger than 10 rpm. For the dynamic characteristic, the output torque behaviors with respect to the step input current are shown in Fig. 9(b). Here, the rotational velocity of the MR rotary actuator is set to 50 rpm. The current is input at the instance of 2 sec, and then removed at the instance of 8 sec. It can be verified that the transient response characteristic of the actuator is nearly independent of the applied current. Especially, considering that the dynamic response of the actuator exhibits similar characteristic to the first order linear system, the time constant of the actuator is found by about 33 msec. Fig. 9(c) shows the experimental results regarding the hysteresis characteristics of the MR fluid actuators, where the output torque are normalized by the measured maximum torque. The rotational velocity of the MR rotary actuator is 50 rpm. The current is varied from 0 through 5 to 0 A, in the triangular waveform with the

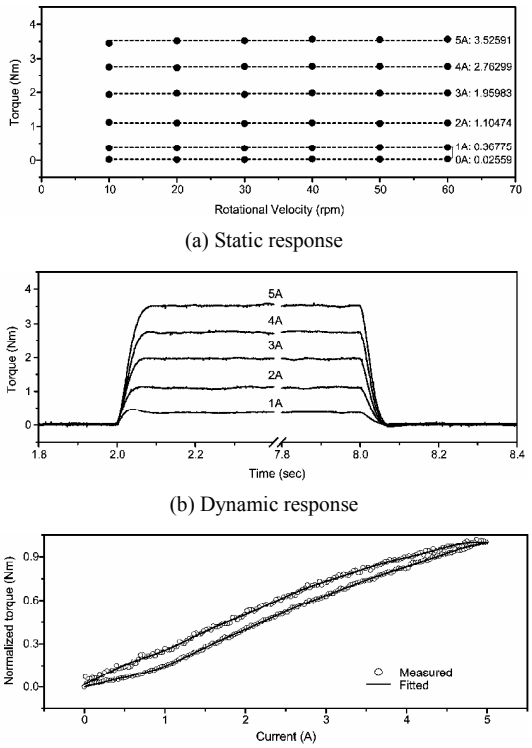

Fig. 9. Structure of the MR rotary actuator.

period of 10 sec. From the result, it is verified that proposed MR rotary actuator has about 10 percent of hysteresis characteristics. Consequently, a series of the experimental results show that the proposed MR rotary actuator can be suitable for the haptic joystick of the virtual excavator simulator in the viewpoint of controllability and fast response.

6. Performance evaluation

The performance evaluation of the proposed virtual excavator simulator is achieved under two conditions: one is the load condition considering the interaction between the soil and the bucket, and the other is the unload condition neglecting the reaction force from the soil. Through the experimental comparison, the effect of the external load on the dynamic behavior of the excavator and the force reflecting performance of the haptic interface is investigated.

6.1 Joystick angle

For generating the trajectory of the bucket tip during digging, the haptic joysticks are manipulated continuously. Fig. 10 shows the joystick angles obtained by the rotary encoders mounted on the MR fluid actuator. To extend the arm and bucket cylinders, the corresponding joysticks are manipulated in the positive angle range. To compress and extend the boom cylinder in succession, the boom joystick is manipulated in the

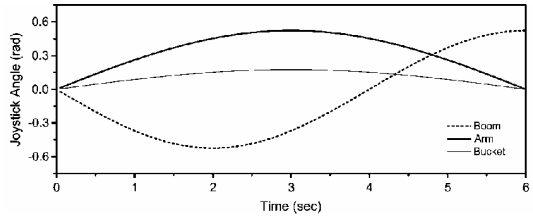

(a) Unload condition

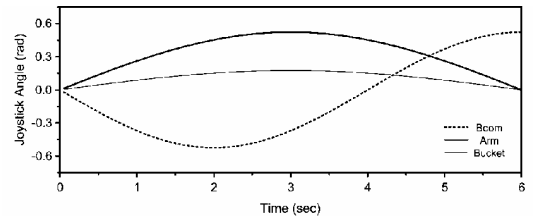

(b) Load condition

Fig. 10. Joystick angles.

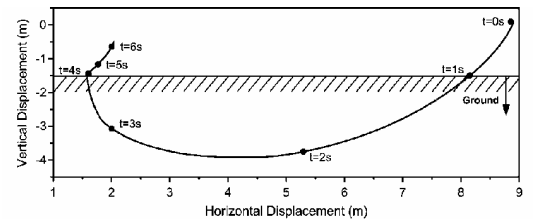

(a) Unload condition

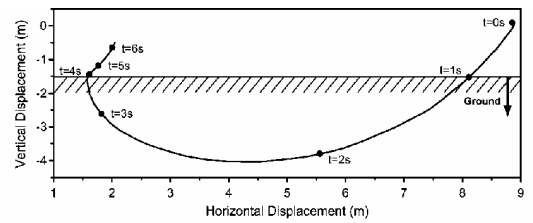

(b) Load condition

Fig. 11. Bucket tip trajectory.

negative and positive direction accordingly. For an effective comparison of the two experiments, a well-trained operator is employed to track the pre-planned joystick angle trajectories. As shown in Fig. 10, the joystick angles in the two experiments are nearly identical. Therefore, it is conceivable that the following experimental results are suitable to compare the performances of the virtual excavator simulator under both load and unload conditions.

6.2 Bucket tip trajectory

Fig. 11 shows the bucket tip trajectories of the virtual excavator for 6 sec. Since swing motion is neglected, the trajectory is on one plane of the reference coordinate system. For convenience, the soil surface is assumed to be horizontal and positioned at the level of -1.5 m. When the bucket tip is placed below the soil surface (1~4 sec), the two trajectories are rather different. It can be considered that the difference in the trajectory during digging results from the interaction effect between the bucket and the soil under the load and unload condition.

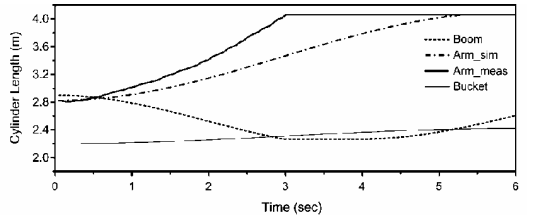

(a) Unload condition

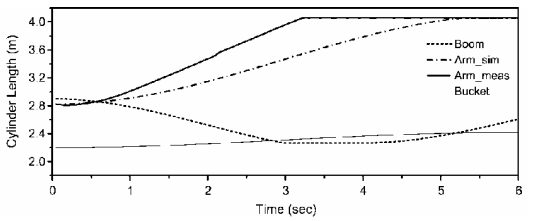

(b) Load condition

Fig. 12. Cylinder lengths.

6.3 Cylinder length

Fig. 12 shows the boom, arm and bucket cylinder lengths. Here, the cylinder length consists of the length of the cylinder itself and the displacement of the piston rod. All of the cylinder lengths are measured in the experiments. In the case of the arm, the cylinder length in the simulation is given by integrating the cylinder velocity proportional to the joystick angle with respect to the time. As shown in Fig. 12, the difference between the measured and simulated lengths is found. Actually, the hydraulic cylinder in hardware is operated by the valve opening area of PDCV corresponding to the joystick angle. However, the valve opening area is not proportional to the displacement of the valve spool or poppet. In other words, the nonlinearity of the hydraulic valve leads to a difference between the measured and simulated length of the arm cylinder. In addition, the arm cylinder is relatively slowly extended under the load condition. It can be considered as the effect of the load applied to the cylinder from the soil.

6.4 Cylinder force

Fig. 13 shows the forces applied to the respective cylinder actuators during digging. In the unload condition, since the soil reaction due to the interaction with the bucket is disregarded, the cylinder forces originate only by the weight and inertia of the link system itself. In the load condition, the system load due to the link operations and the external load due to the soil reaction have an effect on the excavator behavior simultaneously. For that reason, the cylinder forces are differently shown according to the load existence in the time between 1 and 4 sec.

During digging, the forces of the arm and bucket cylinders

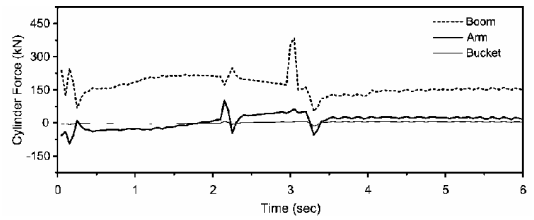

(a) Unload condition

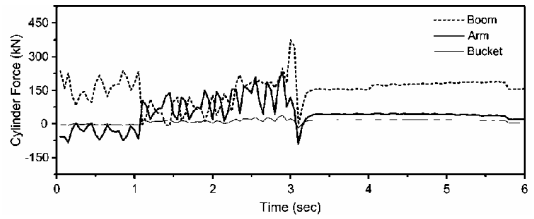

(b) Load condition

Fig. 13. Cylinder forces.

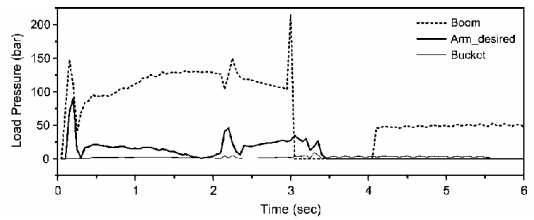

(a) Unload condition

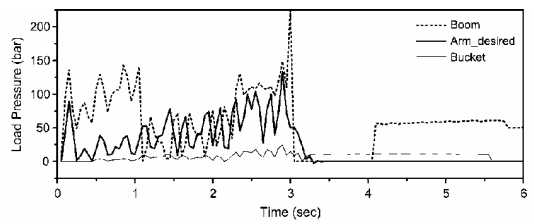

(b) Load condition

Fig. 14. Cylinder load pressures.

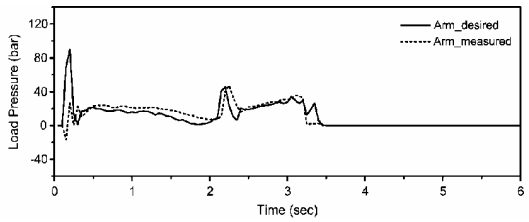

(a) Unload condition

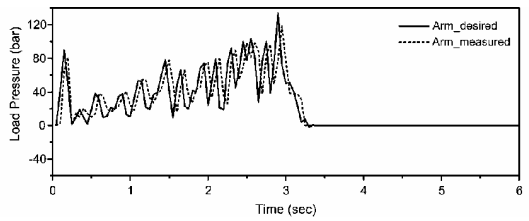

(b) Load condition

Fig. 15. Calculated and measured load pressures in the arm cylinder.

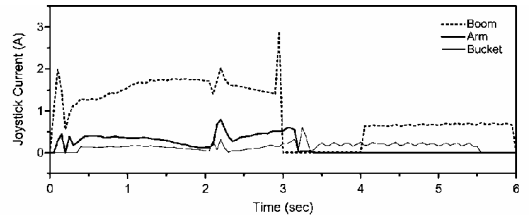

(a) Unload condition

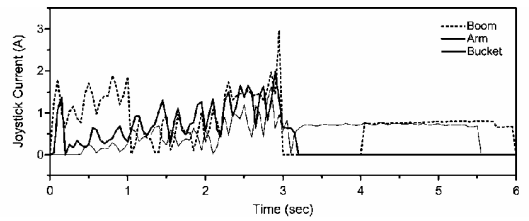

(b) Load condition

Fig. 16. Joystick currents.

are increased, whereas the boom cylinder force is relatively decreased. The boom cylinder plays a role supporting the whole manipulator, including the arm and the bucket. In the load condition, the weight of the manipulator is compensated by the soil reaction, leading to the reduction of the boom cylinder force. Contrarily, the arm and bucket cylinder forces have more effect on the soil reaction than the weight compensation, which is due to the geometric configuration of the manipulator. Especially, the force chattering during the digging is considered to be caused by the dynamic characteristic of the hydraulic system due to the compressibility of the working oil. Therefore, the dynamic behavior of the real hydraulic system is effectively reflected to the virtual excavator simulator via HILS technology.

6.5 Cylinder load pressure

The cylinder load pressures of the virtual excavator are shown in Fig. 14. Since the used cylinders are single-ended type, the cylinder pressures during the extension or compression are different due to different piston areas. The cylinder load pressure shows a similar tendency to the corresponding cylinder force in Fig. 13, but it remains positive always. The PPRV in the HILS system is placed between the return port of PDCV and the tank. With the arrangement, the pressure control input to the PPRV is always positive, regardless of the operating direction of the cylinder. In other words, the cylinder load pressure is activated against the movement of the cylinder, which provides a similar effect to the passivity effect of the MR rotary actuator in the haptic joystick.

On the other hand, Fig. 15 shows the desired and measured load pressure in the arm cylinder. In both experimental conditions, the measured load pressure is relatively well tracking the desired, in spite of a little phase lag, which is caused by the dynamic response of the PPRV. With the improved control algorithm, the tracking error can be reduced to the desired

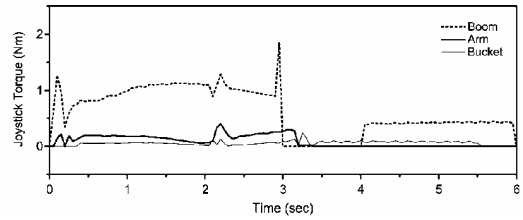

(a) Unload condition

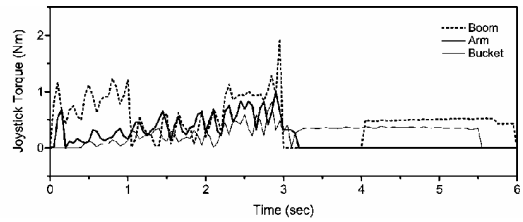

(b) Load condition

Fig. 17. Joystick torques.

extent in such a way that the development of the simulator with further reality is also possible.

6.6 Joystick current and torque

Fig. 16 shows the current inputs to the MR rotary actuators corresponding to the cylinder load pressures. Fig. 17 shows the torque outputs of the MR rotary actuators which are obtained by the relations of the static and dynamic characteristics. Considering that the torque outputs are very similar to the cylinder load force trajectories in Fig. 14, we expect that the excavator operator can perceive the force feedbacks by the haptic joysticks effectively.

7. Conclusions

We have proposed the technical concept of the virtual excavator simulator featuring HILS technology and haptic joysticks.

The mathematical relations describing the excavator operation in the simulation environment have closed solutions in such a way that real-time implementation can be achieved without numerical analysis requiring computational burden and convergent error. Considering the nonlinearity of the hydraulic system and the complex modeling due to the parameter uncertainty, the HILS system is constructed by integrating the real hydraulic system with the excavator simulation environment. Therefore, the virtual excavator simulator reflects the dynamic characteristics of the hydraulic system effectively. A haptic joystick is proposed for the bilateral information transmission between the operator and the virtual excavator. Haptic stability and interface safety in the haptic joystick are concurrently guaranteed by the MR rotary actuator, which is characterized by simple structure, high power density, low inertia and passivity property. Through the performance evaluation, it is verified that the proposed virtual excavator simulator is effective and practical from the viewpoint of reality improvement.

Acknowledgment

This work was supported for two years by Pusan National University Research Grant.

References

[1] L. E. Bernold, L. Venkatesan and S. Suvarna, A multi-sensory approach to 3-D mapping of underground utilities, *Proc. of the 19th International Symposium on Automation and Robotics in Construction*, Gaithersburg, Maryland, USA (2002) 525-530.

[2] P. Lever, F. Wang and D. Chen, A fuzzy control system for an automated mining excavator, *Proc. of the International Conference on Robotics and Automation*, San Diego, CA, USA, 4 (1994) 3284-3289.

[3] A. Stentz, A. Kellyy, P. Randerz, H. Herman, O. Amidi, R. Mandelbaum, G. Salgianx and J. Pedersen, *Real-time, multi-perspective perception for unmanned ground vehicles*, Robotics Institute, Carnegie Mellon University, USA (2003).

[4] A. J. Koivo, M. Thoma, E. Kocaoglan and J. Andrade-Cetto, Modeling and control of excavator dynamics during digging operation, *J. of Aerospace Engineering*, 9 (1) (1996), 10-18.

[5] Q. He, D. Zhang, P. Hao and H. Zhang, Modeling and controlling for hydraulic excavator's arm, *Proc. of the 22nd International Symposium on Automation and Robotics in Construction*, Ferrara, Italy (2005) 1-6.

[6] Q. P. Ha, Q. H. Nguyen, D. C. Rye and H. G. Durrant-Whyte, Impedance control of a hydraulically actuated robotic excavator, *Automation in Construction*, 9 (5-6) (2000) 421-435.

[7] N. R. Parker, S. E. Salcudean and P. D. Lawrence, Application of force feedback to heavy duty hydraulic machines, *Proc. of the IEEE International Conference on Robotics and Automation*, Atlanta, USA, 1 (1993) 375-381.

[8] J. G. Frankel, M. E. Kontz and W. J. Book, Design of a test-bed for haptic control of hydraulic systems, *Proc. of ASME International Mechanical Engineering Congress and Exposition*, Anaheim, USA (2004).

[9] A. Takemoto, K. Yano, T. Miyoshi and K. Terashima, Operation assist control system of rotary crane using proposed haptic joystick as man-machine interface, *Proc. of the 13th IEEE International Workshop on Robot and Human Interactive Communication*, Kurashiki, Japan (2004) 533-538.

[10] S. Y. Yang, S. K. Kwon and S. M. Jin, Hydraulic simulation and remote control system of field robot, *Proc. of the 10th International Conference on Control, Automation, Robotics and Vision*, Hanoi, Vietnam (2008) 2303-2308.

[11] S. P. DiMaio, S. E. Salcudean, C. Reboulet, S. Tafazoli and K. Hashtrudi-Zaad, A virtual excavator for controller development and evaluation, *Proc. of the IEEE international Con-*

ference on Robotics and Automation, Leuven, Belgium, 1 (1998) 52-58.

[12] H. I. Torres-Rodriguez, V. Parra-Vega and F. J. Ruiz-Sanchez, Integration of force-position control and haptic Interface facilities for a virtual excavator simulator, *Proc. of the 12th International Conference on Advanced Robotics*, Seattle, WA, USA (2005) 761-768.

[13] R. N. Yong and A. W. Hanna, Finite element analysis of plane soil cutting, *J. of Terramechanics*, 14 (3) (1977) 103-125.

[14] O. luengo, S. Singh and H. Cannon, Modeling and identification of soil-tool interaction in automated excavation, *Proc. of IEEE/RSJ International Conference on Intelligent Robotic Systems*, Victoria, USA, 3 (1998) 1900-1906.

[15] Y. J. Nam, Y. J. Moon and M. K. Park, Performance improvement of a rotary MR fluid actuator based on electromagnetic design, *J. of Intelligent Material Systems and Structures*, 19 (6) (2008) 695-705.

Yun-Joo Nam received the Ph.D. from Pusan National University, Busan, Korea. He is currently a senior researcher of Construction Equipment Technology R&BD group in Korea Institute of Industrial Technology.

Myeong-Kwan Park received the M.S. and Ph.D. degrees from Tokyo Institute of Technology, Tokyo, Japan. He is currently a full professor in the Department of Mechanical Engineering and a researcher in the Research Institute of Mechanical Technology, at Pusan National University.